

# The Effect of the Thickness of the Porous Material On The Parallel Plate Channel Flow of A Jeffrey Fluid When One The Walls are Provided with Porous Lining

**G Sunil Babu**

Department of Mathematics, Sri Venkateswara University, Tirupati, India

**S Sreenadh**

Department of Mathematics, Sri Venkateswara University, Tirupati, India

**G Gopi Krishna**

Department of Mathematics, MarriLaxman Reddy Institute of Technology & Management, Dundigal, Hyderabad, India

**S.R. Mishra**

Department of Mathematics, Siksha 'O' Anusandhan, Bhubaneswar, Odisha, India

*Abstract*-Presently, the stream past a deformable permeable channel limited by the limited deformable permeable layer with unbending equal plates is explored. The coupled overseeing conditions are addressed scientifically, and the definition of the wooden speed field, liquid speed, and strong removal are acquired. The impacts of the retentive layer thickness and the drag on the stream dislodging and rate are analyzed graphically. It is found that removal increments with rising drag, while the elective behaviors in the speed. It is seen that they present the retard in rate with extending consistency boundaries.

Index Terms - *Porous layer; viscous flow; Jeffrey fluid; porous layer thickness*

## *Phraseology*

$x, y$	<i>The rectangular cartesian coordinates</i>
$\mu$	<i>The Lamé constant</i>
$\mu_a$	<i>The apparent viscosity of the fluid in the porous material</i>
$K$	<i>The drag coefficient</i>
$\mu_f$	<i>The coefficient of viscosity</i>
$v$	<i>The velocity of the fluid through the rigid deformable layers</i>
$h$	<i>width of the wall</i>
$\varepsilon$	<i>Porous layers thickness</i>
$u$	<i>The displacement</i>
$\phi$	<i>The volume fraction of the fluid</i>
$\delta$	<i>Viscous drag</i>
$\frac{\partial p}{\partial x} = G_0$	<i>Typical pressure gradient</i>
$q$	<i>Fluid velocity in free flow</i>
$\lambda_1$	<i>Jeffrey parameter</i>

## INTRODUCTION

Fluid flow through soft, deformable solid surfaces happens in various settings: biological systems include fluid flow via tubes with flexible walls. Specific biotechnological applications involve fluid flow past polymer matrices and membranes because of the connection between fluid and solid dynamics, fluid flow dynamics through deformable solids different qualitatively from rigid surfaces. The solid elasticity can affect the fluid flow. In the fields of medicine and geology, viscous flow and via a porous medium has numerous essential uses.

The more critical investigation works accessible inflow through permeable media is chiefly focused on the undeformable permeable media. Yet, when we consider marvels, for example, hemodynamic impacts of the endothelial glycocalyx, the hypothesis of undeformable permeable media is deficient to clarify the bio-liquid conduct. The conjoined liquid stream and deformation marvel of permeable substances is an issue of prime importance in natural delicate tissue displaying, and skin myocardium geomechanics biomechanics incorporates ligament and blood vessel dividers.

In geomechanics, Biot [1] projected a technique for simulating deformable porous medium utilizing mixture theory. After this method was used in various biomechanics applications, including skin, arytenoid, bone, articular permeability, etc., Mow et al. [2] gave an magnificent analysis of the fluid flow articular cartilage mechanical characteristics concerning mixture theory. Channabasappa et al. [3] discussed the porous substance thickness on the parallel plate channel flow with an absorbent lining. Oomens et al. [4] explored a mixture strategy to the functions of skin.

Huyghe et al. [5] examined a finite element two-phase modeling of the left diastolic ventricle. Kenyon [6] extensively worked on a mathematical model of aortic tissue water flow. Rudraiah [7] has explored impermeable parallel flows in a channel with a finite-thickness porous material bounding one another. Jayaraman [8] has described in theoretical investigation of water transport in the arterial wall. Yang et al. [9] exposed in cardiac muscle, the conduct of evident viscoelastic for-poroelasticity is considered. Huyghe et al. [10] observed a "two-phase finite element model" of the left diastolic ventricle.

Klanchar et al. [11] are examined modeling water flow via arterial tissue. Ahmed and Siddique [12] proposed a flow-induced deformable porous material mathematical model with an identical magnetic field assumption.

In these models, the fluid flows by a porous deformable layer. Barry et al. [13] and Ranganatha&Siddagamma [14] found the correct solution to analyze the unsteady viscous flow across a deformable porous layer using the theory of mixtures. Sreenadh et al. [15-18] have studied mathematical models that were influencing deformable porous medium.

In context on the above assessments, when the dividers are provided with porous surface, the influence of the thickness of the permeable material on the equal plate channel stream of a Jeffrey fluid The liquid speed and removal of the strong network are assessed. Tables and charts are utilized to represent the effects of different actual elements on stream attributes.

## MATHEMATICAL MODELLING

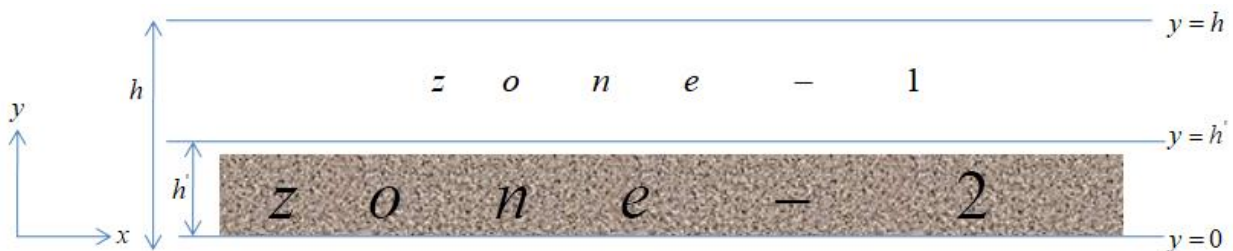


**Fig 1: Schematic Diagram**

Let us consider a fluid flowing through a deformable porous layer. These are bounded between two layers, i.e.,  $y = h'$  and  $y = h$ ; thickness of deformable membrane  $y = h'$  attached to the lower walls, as shown in Fig.1. They divided the flow between the two layers into two parts. It formed the deformable porous layer among the interface of  $y = 0$ ,  $y = h'$  and  $y = h'$ ,  $y = h$  in the free flow layer. The deformation of the solid matrix is  $(u, 0, 0)$ . We assume the fluid velocity to be  $(v, 0, 0)$  and free flow velocity  $(q, 0, 0)$ . The pressure gradient  $\frac{\partial p}{\partial x} = G_0$  is applied to develop an axially directed flow in the channel.

In perspective on the suppositions referenced over, the conditions of movement in the free section and deformable permeable layer are (See for details Barry et al. [13]).

$$\mu \frac{\partial^2 u}{\partial y^2} - (1 - \phi) G_0 + K v = 0 \tag{1}$$

$$\frac{2\mu_a}{1+\lambda_1} \frac{\partial^2 v}{\partial y^2} - \phi G_0 - K v = 0 \quad (2)$$

$$\frac{\mu_f}{1+\lambda_1} \frac{\partial^2 q}{\partial y^2} = G_0 \quad (3)$$

We utilize the following systematic group of quantities for non-dimensionalization

$$\frac{y}{h} = y^*, u^* = \frac{-\mu u}{h^2 G_0}, v^* = \frac{-\mu_f v}{h^2 G_0}, q^* = \frac{-\mu_f q}{h^2 G_0}, \varepsilon = \frac{h^1}{h}, \delta = \frac{K h^2}{\mu_f}, \eta = \frac{\mu_f}{2\mu_a}$$

The governing equations (1)-(3) become (after dropping \*)

$$\frac{d^2 u}{dy^2} = -(1-\phi) - \delta v \quad (4)$$

$$\frac{d^2 v}{dy^2} - (1+\lambda_1) \delta \eta v = -\phi(1+\lambda_1) \eta \quad (5)$$

$$\frac{d^2 q}{dy^2} = -(1+\lambda_1) \quad (6)$$

The differential equations from Eq(4) to Eq(6) are solved by using the following boundary conditions:

$$\left. \begin{aligned} v(y) = 0, u(y) = 0 \text{ when } y = 0 \\ q(y) = \phi v, \frac{dq}{dy} = \frac{1}{(1-\phi)} \frac{du}{dy} \text{ when } y = \varepsilon \\ \frac{dq}{dy} = \frac{1}{\eta\phi} \frac{dv}{dy} \text{ when } y = \varepsilon \\ q(y) = 0 \text{ when } y = 0 \end{aligned} \right\} \quad (7)$$

### SOLUTION OF THE PROBLEM

The differential conditions of Eq (4) and Eq (6) are together with boundary conditions that may be solved using Eq (7). The following are the solid displacement and fluid velocity in the free flow layer and deformable permeable layer:

$$u(y) = -\frac{y^2}{2} - \frac{c_1 \delta}{a^2} e^{ay} - \frac{c_2 \delta}{a^2} e^{-ay} + c_3 y + c_4 \quad (8)$$

$$v(y) = c_1 e^{ay} + c_2 e^{-ay} + \left( \frac{\phi^f}{\delta} \right) \quad (9)$$

$$q(y) = \frac{-(1+\lambda_1)y^2}{2} + c_5 y + c_6 \quad (10)$$

Where  $a = \sqrt{\delta\eta(1+\lambda_1)}$ ,  $b = -\phi(1+\lambda_1)\eta$

$$c_6 = (1+\lambda_1)(0.5-\varepsilon) - \frac{a}{\eta\phi} (c_1 e^{a\varepsilon} - c_2 e^{-a\varepsilon})$$

$$c_5 = (1 + \lambda_1) \varepsilon + \frac{a}{\eta \phi} (c_1 e^{a\varepsilon} - c_2 e^{-a\varepsilon})$$

$$c_3 = [c_1 e^{a\varepsilon} - c_2 e^{-a\varepsilon}] \left( \frac{a(1-\phi)}{\eta \phi} \right) + \frac{\delta}{a} + \varepsilon$$

$$c_1 = \frac{1}{\left\{ e^{a\varepsilon} \left[ \phi - \frac{a(\varepsilon-1)}{\eta \phi} \right] - e^{-a\varepsilon} \left[ \phi + \frac{a(\varepsilon-1)}{\eta \phi} \right] \right\}} \left\{ \left( \frac{1+\lambda_1}{2} \right) + (1+\lambda_1) \left( \frac{\varepsilon^2}{2} - \varepsilon \right) + \frac{\phi e^{-a\varepsilon}}{\delta} \left[ \phi + \frac{a(\varepsilon-1)}{\eta \phi} \right] - \frac{\phi^2}{\delta} \right\}$$

$$c_2 = \frac{1}{\left\{ e^{a\varepsilon} \left[ \phi + \frac{a(\varepsilon-1)}{\eta \phi} \right] - e^{-a\varepsilon} \left[ \phi - \frac{a(\varepsilon-1)}{\eta \phi} \right] \right\}} \left\{ \left( \frac{1+\lambda_1}{2} \right) + (1+\lambda_1) \left( \frac{\varepsilon^2}{2} - \varepsilon \right) + \frac{\phi e^{a\varepsilon}}{\delta} \left( \phi - \frac{a(\varepsilon-1)}{\eta \phi} \right) - \frac{\phi^2}{\delta} \right\}$$

$$c_4 = \frac{-\phi}{a^2}$$

#### 4. RESULTS AND DISCUSSION

We examine the steady effect of the porous material's thinness on the equal channel stream of a Jeffrey fluid when the dividers are presented with penetrable adjusting in this article. The consequences are put in a kind word for various parameters like the volume fraction of the fluid  $\phi$ , viscosity parameter  $\eta$ , thickness  $\varepsilon$ , drag  $\delta$ , and Jeffrey parameter  $\lambda_1$ . In this, we observed the numerical computation we used  $\phi = 0.6, \delta = 1, \eta = 0.5, \varepsilon = 0.2$  and  $\lambda_1 = 0.5$ . They save these values as not unusual inside the complete study besides for different values as displayed in fig 2 to 15.

From the Equation (10) the velocity  $q$  is computed with  $y$  and the following changes are noticed in figures 2,3,4, and 5 for different values of  $\eta, \lambda_1, \phi$  and  $\varepsilon$ . They illustrate the impact of  $\eta$  on free flow velocity in fig.2, by doing so it exposes the free flow velocity increases as  $\eta$ . By increasing Jeffrey parameter, the free flow velocity also raises, which is explained in fig.3.

With the increase in volume fraction  $\phi$  one can visualise that the free flow velocity decreases from fig.4. From figure 5, the free flow velocity reduces with the increased porous layer thickness  $\varepsilon$ .

They illustrate the impact of  $\eta$  on free flow velocity in fig.2, by doing so it exposes the free flow velocity increases as  $\eta$ . By increasing Jeffrey parameter, the free flow velocity also raises, which is explained in fig.3. With the increase in volume fraction  $\phi$  one can visualise that the free flow velocity decreases from fig.4. From figure 5, the free flow velocity reduces with the increased porous layer thickness  $\varepsilon$ .

Using the distinct values of  $\phi, \eta, \lambda_1, \varepsilon$  and  $\delta$ , one can understand the modern approach of flow velocity  $v$  in the deformable porous layer with  $y$  and they are manifested in figures 6,7,8,9 and 10. It is clearly observed that by increasing volume fraction  $\phi$  and viscous parameter  $\eta$  the velocity of the fluid flow increased. It is noticed that the flow rate increases by proliferating the Jeffrey parameter  $\lambda_1$  and it is pictured in figure 8. Figure 9 indicates that the flow rate magnify as porous layer thickness  $\varepsilon$  rises. It is evidently noticed from figure 10 that the flow velocity and drag had opposite behaviour i.e. whenever the drag  $\delta$  increases then the flow velocity decreases.

From equation 8, we evaluated the different variations of solid displacement  $u(y)$  for distinct qualities of physical quantities of  $\phi, \eta, \lambda_1, \varepsilon$  and  $\delta$  are portrayed in figures 11,12,13,14, and 15. From figure 11 it enhanced influence of the thickness parameter with increasing solid displacement. In figures 12 and 13 we display that the substantial removal will increase with drag  $\delta$  and Jeffrey parameter  $\lambda_1$ . From figures 14 and 15, one can evidently observed that when the volume fraction of the fluid  $\phi$  and the viscosity parameter  $\eta$  are growing, then the rigid deformable flow and flow rate diminishes.

The difference in volume flow velocity between rigid deformable and flow free flow  $Q_D (0 \leq v(y) \leq 1)$  for outstanding values of different physical parameters  $\delta, \eta, \varepsilon,$  and  $\phi$  and is explained in table 1, by comparing with fixed  $\lambda_1 = 0.2$ . It is unmistakable

that the significance of amount volume flow rate  $Q_D(0 \leq v(y) \leq 1)$  with a permeable medium which is deformable is lessen with expansion in the significance of thickness parameter  $\varepsilon$ , drag parameter  $\delta$  for constant value of Jeffrey parameter  $\lambda_1 = 0.2$ . It is additionally seen that the upsides of volume flow rate with deformable permeable medium advancements with rising upsides of volume part and consistency boundary for a decent worth of Jeffery parameter  $\lambda_1 = 0.2$ .

Table II illustrates that the rigid flow version in  $Q_{D1}(0 \leq v(y) \leq 1)$  volume flow rate with distinct values of the physical parameters  $\delta, \eta, \text{ and } \phi$  and all the table values assessed for standard value  $\lambda_1 = 0.2$ . Further, for fixed Jeffrey parameter  $\lambda_1 = 0.2$  and by increasing the different physical parameters  $\delta, \eta$ , we clearly observe that the importance of volume flow velocity  $Q_{D1}(0 \leq v(y) \leq 1)$  with pleomorphic porous medium the various values of volume flow rate are growing with increasing values of  $\phi$ , for fixed  $\lambda_1 = 0.2$ .

## CONCLUSIONS

This paper surveyed the slimness of the equal stream channel of the penetrable material of a Jeffrey liquid when the dividers gave permeable covering. The outlines show the effect of various actual elements on strong dislodging, liquid speed, and free stream rate.

- 1) The liquid speed diminishes with expanding upsides of drag. The contrary conduct is seen for the volume part of the fluid.
- 2) The penetrable layer thickness in the channel with rate redesigns with growing potential gains of porous layer thickness.

## REFERENCES

- [1] Biot M A. General theory of three-dimensional consolidation. J. Appl. Phys. 1941; 12:155-164.
- [2] Mow VC, Holmes MH, Lai M. Fluid transport and mechanical properties of articular cartilage: a review. J. Biomechanics 1984; 17: 377-394.
- [3] Channabasappa M N., Umapathy K G and Nayak I V ., The effect of the thickness of the porous material on the parallel plate channel flow when the walls are provided with non-erodible porous lining, Appl.Sci.Res. 32, 607-617, (1976).
- [4] Oomens C.W.J, Van Campen D.H, and Grootenboer H.J, A mixture approach to the mechanics of skin, J.Biomech.20,877-885,(1987)
- [5] Huyghe J.M, Van Campen D. H, Arts T and Heethaar R.M, A two-phase finite element model of the diastolic left ventricle, J. Biomech. 24, 527-538, (1991)
- [6] Kenyon D.E, A mathematical model of water flux through aortic tissue, Bull.Math. Biol.41, 79-90, (1979).
- [7] Rudraiah., N., Coupled parallel flow in a channel and a bounding porous medium of finite thickness, Transaction of the ASME, vol.107, 322-329, (1985).
- [8] Jayaraman G, Water transport in the arterial wall- A theoretical study, J.Biomech. 16, 833-840, (1983).
- [9] Yang M and Taber L A., The possible role of poroelasticity in the apparent viscoelastic behavior of passive Cardiac muscle, J.Biomach, 24(7), 587-97, 1991.
- [10] J H Huyghe., Dick H Van Campen., Theo Arts and Robert M Heethaar., A two-phase finite element model of the diastolic left ventricle, Journal of Biomechanics, 24(7), 527-538, 1991.
- [11] Klanchar M and Tarbell J. M, Modelling water flow through arterial tissue, Bull. Math.Biol. 49, 651-669, (1987)
- [12] A. Ahmed, J. I. Siddique, The effect of magnetic field on flow induced-deformation in absorbing porous tissue, Math. Biosci. & Eng., 16(1) (2019) 1-17.
- [13] Barry SI, Parker KH, Aldis GK. Fluid flow over a thin deformable porous layer, Journal of Applied Mathematics and Physics (ZAMP) 1991; 42: 633-648.
- [14] Ranganatha T R, Siddagamma NG. The flow of Newtonian fluid a channel with deformable porous walls. Proc. of National Conference on Advances in fluid mechanics 2004;49-57.
- [15] Sreenadh S, Krishnamurthy M, Sudhakara E, GopiKrishna G. Couette flow over a deformable permeable bed, (IJIRSE) International Journal of Innovative Research in Science & Engineering 2014; ISSN(Online) 2347-3207.
- [16] Sreenadh S, Prasad K V, Vaidya, H, M, Sudhakara E, GopiKrishna G, Krishnamurthy M., MHD Couette flow of a Jeffrey fluid over a deformable porous layer, Int. J. Appl.Comput. Math, 2016. DOI 10.1007/s40819-016-0232-1.
- [17] Sreenadh S, Krishnamurthy M, Sudhakara E, GopiKrishna G, Venkateswarlu Naidu, D., MHD free surface flow of a Jeffrey fluid over a deformable porous layer, Global Journal of Pure and Applied Mathematics, Vol (11), 2015, 3889-3903
- [18] Sreenadh, S., Rashidi, M.M., Kumara Swami Naidu, K., Parandhama A., Free Convection flow of a Jeffrey fluid through a vertical Deformable porous Stratum, JAFM, 2391- 2401, 2015.

**Table I: For fixed value  $\lambda_1 = 0.2$**

$\delta$	$\phi$	$\eta$	$\varepsilon$	$Q_D$
1	0.6	0.5	0.2	0.0631
2				0.0630
3				0.0629
4				0.0628
1	0.2			0.0534
	0.4			0.0574
	0.6			0.0631
	0.8			0.0700
	0.6	0.333		0.0592
		0.666		0.0667
		1		0.0738
		0.5	0.1	0.0786
			0.2	0.0631
			0.3	0.0528

**Table II: For fixed value  $\lambda_1 = 0.2$**

$\delta$	$\phi$	$\eta$	$Q_{D1}$
1	0.6	0.5	1.6481
2			1.0286
3			0.8110
1	0.2		0.8670
	0.4		1.2575
	0.6		1.6481
	0.8		2.0387
	0.6	0.333	1.6648
		0.666	1.6322
		1	1.6018

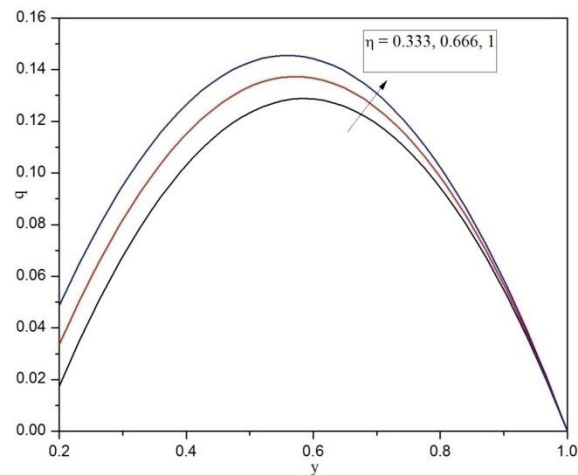


**Figure 2: Profiles of free flow velocity for various values of  $\eta$**

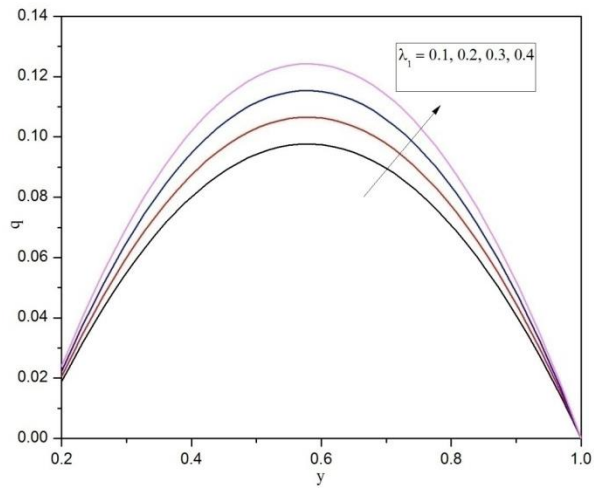


Figure 3: free flow velocity profiles for specific quantities of  $\lambda_1$

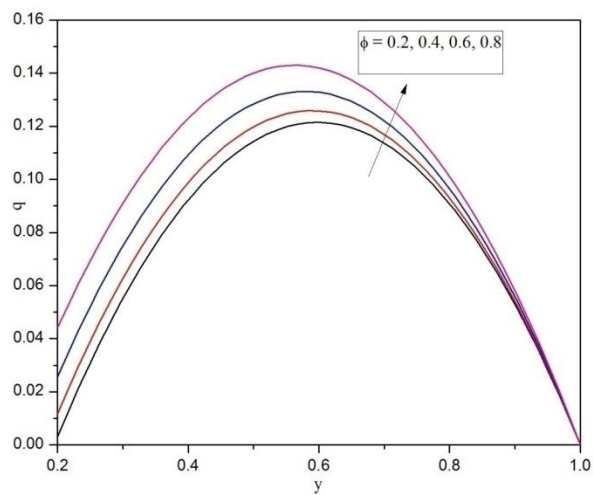


Figure 4: Profiles of free flow velocity for various quantities of  $\phi$

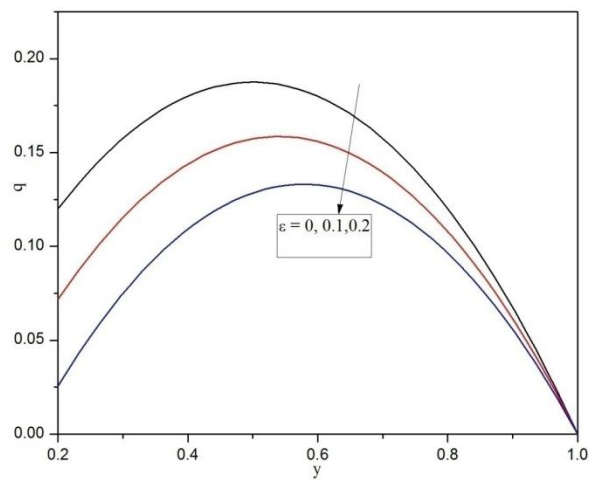
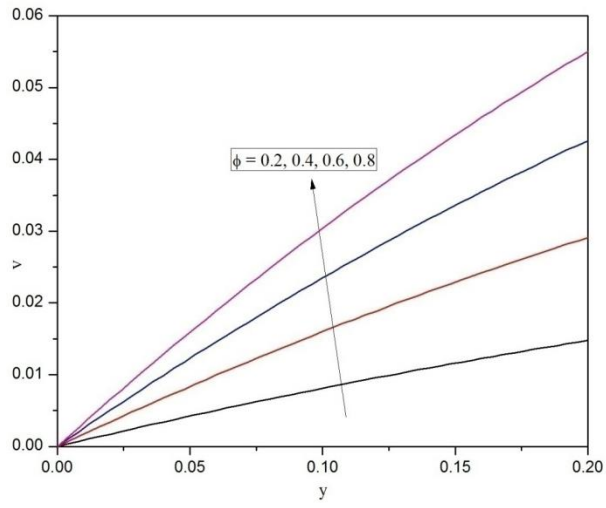
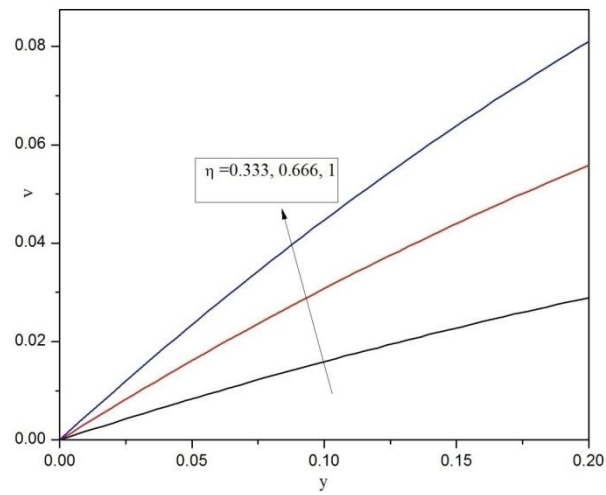


Figure 5: free flow velocity profiles for specific quantities of  $\epsilon$



**Figure 6: velocity structures for distinct qualities of  $\phi$**



**Figure 7: velocity profiles for particular qualities of  $\eta$**

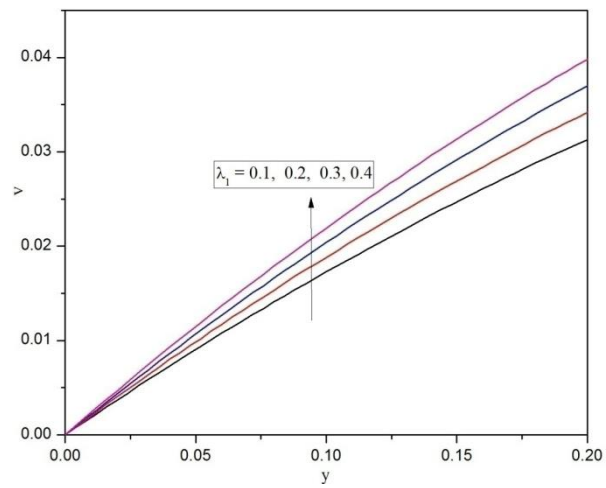


**Figure 8: velocity profiles for various qualities of  $\lambda_1$**



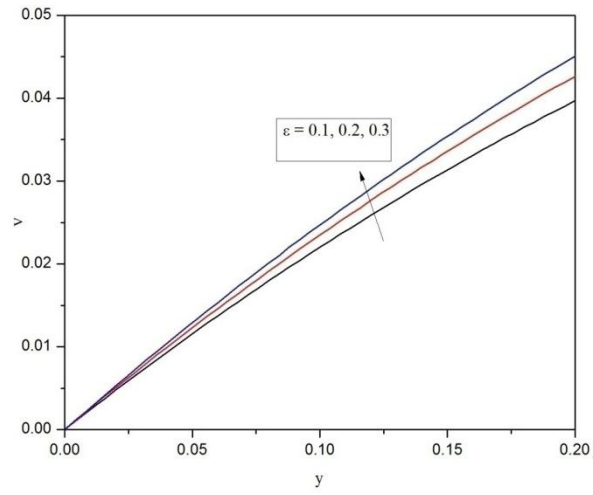


**Figure 9: velocity profiles for various quantities of  $\varepsilon$**

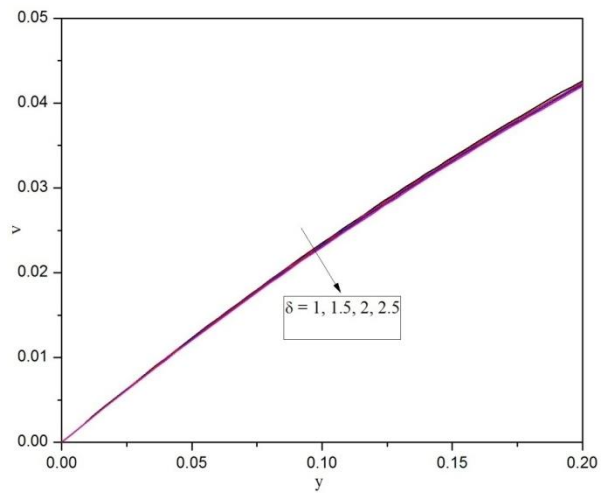


**Figure 10: velocity profiles for various quantities of  $\delta$**

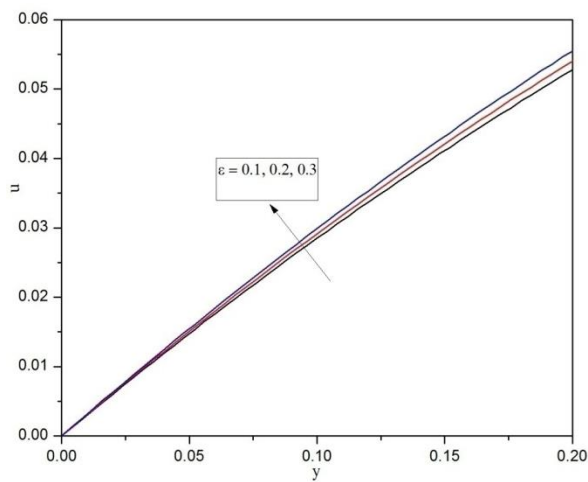


**Figure 11: Displacement profiles for various quantities of  $\varepsilon$**

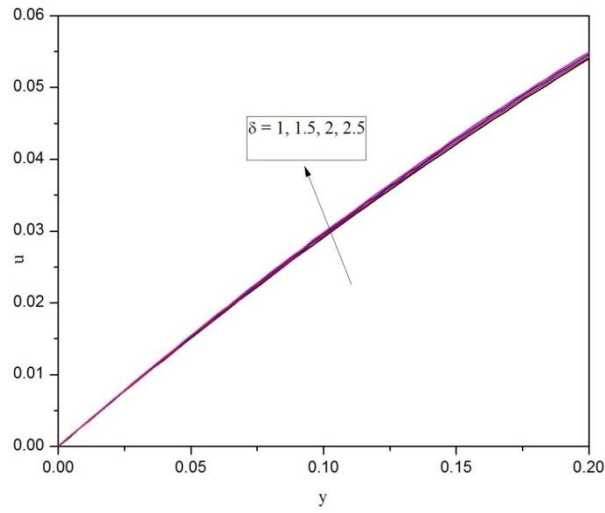


**Figure 12: Displacement profiles for distinct qualities of  $\delta$**

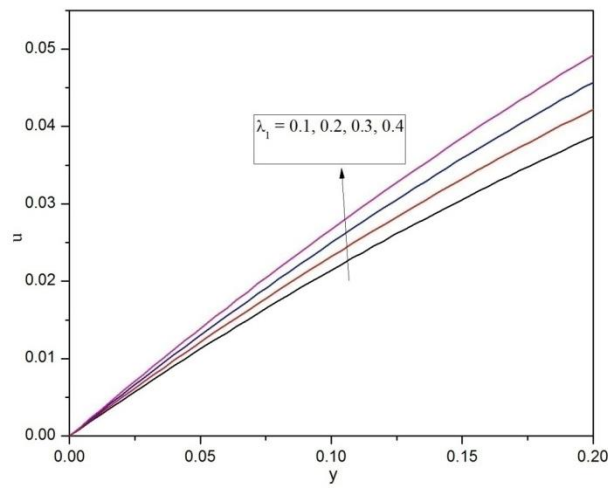


**Figure 13: Displacement profiles for various quantities of  $\lambda_1$**

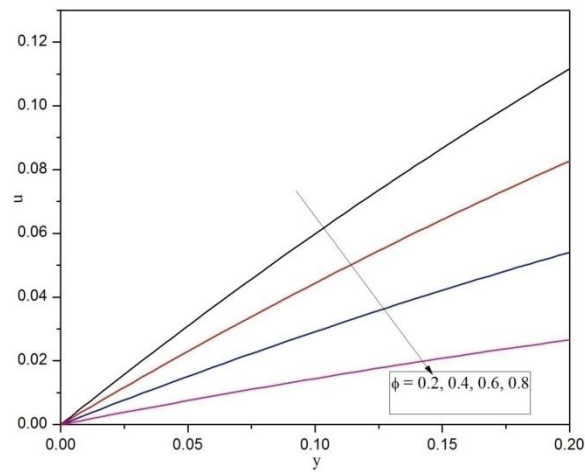


**Figure 14: Displacement profiles for distinct quantities of  $\phi$**

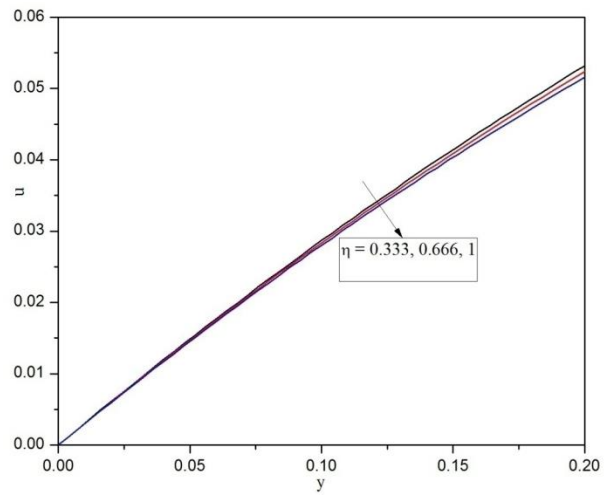


**Figure 15: Displacement profiles for various quantities of  $\eta$**